

MIXED CONVECTIVE SLIP FLOWS IN A VERTICAL PARALLEL PLATE MICROCHANNEL WITH SYMMETRIC AND ASYMMETRIC WALL HEAT FLUXES

Hamid Niazmand, Behnam Rahimi
Department of Mechanical Engineering, Ferdowsi University of Mashhad, Mashhad, Iran.
E-mail: niazmand@um.ac.ir

Received August 2011, Accepted November 2012
No. 11-CSME-66, E.I.C. Accession 3306

ABSTRACT

Mixed convective gaseous slip flows in an open-ended vertical parallel-plate channel with symmetric and asymmetric wall heat fluxes are numerically investigated. Buoyancy effects on developing and fully developed solutions are studied using the SIMPLE algorithm. The velocity and temperature fields are examined for different values of Knudsen number, mixed convection parameter and heat flux ratio. It is found that increasing Gr/Re leads to an increase in the heat transfer rate and friction coefficient. Also, rarefaction effects decrease the heat transfer rate and friction coefficient. The friction coefficient decreases with an increase in heat flux ratio.

Keywords: mixed convection; rarefaction effects; microchannel; SIMPLE algorithm.

CONVECTION MIXTE D'UN ÉCOULEMENT GLISSANT DANS UN MICROCANAL À PAROIS VERTICALES PARALLÈLES AVEC FLUX THERMIQUES SYMÉTRIQUE ET ASYMÉTRIQUE

RÉSUMÉ

La convection mixte d'un écoulement gazeux glissant dans un microcanal ouvert à parois verticales parallèles avec flux thermique symétrique et asymétrique est étudiée numériquement. Les effets de flottabilité sur les solutions en développement ou complètement développées sont traités à l'aide de l'algorithme SIMPLE. Les champs de vitesse et de température sont examinés pour les différentes valeurs de nombres KNUDSEN, de paramètres de convection mixte et du ratio du flux thermique. On constate que l'augmentation de Gr/Re conduit à une augmentation du taux de transfert thermique et du coefficient de frottement. En outre, les effets de la raréfaction diminuent le taux de transfert thermique et le coefficient de frottement. Le coefficient de frottement diminue avec une augmentation du ratio du flux thermique.

Mots-clés : convection mixte ; effets de la raréfaction ; microcanal ; algorithme SIMPLE.

NOMENCLATURE

c_p	specific heat at constant pressure
D	channel width
D_h	hydraulic diameter
g	gravitational acceleration
Gr	Grashof number
H	channel height
K	Thermal conductivity
Kn	Knudsen number
Nu	local Nusselt number
p	pressure
q	local heat transfer rate (heat flux)
r_q	heat flux ratio
Re	Reynolds number
T	temperature, K
u	velocity components in x direction, m/s
U	dimensionless velocity component in x direction
v	velocity components in y directions, m/s
V	dimensionless velocity component in y direction
x, y	coordinate system
X, Y	dimensionless coordinate system
Greek symbols	
β	thermal expansion coefficient
γ	specific heat ratio
Γ	dimensionless local friction coefficient
θ	dimensionless temperature
λ	molecular mean free path
μ	dynamic viscosity
ρ	density
σ_t	thermal accommodation coefficient
σ_v	tangential momentum accommodation coefficient
Subscripts	
0	ambient values
c	cold wall
h	hot wall
g	gas value near the wall surface
m	mean temperature
s	slip/jump values
w	wall values

1. INTRODUCTION

In recent years, fluid flow and heat transfer in microscale devices have become an important research topic due to the rapid growth of practical applications in microelectromechanical systems (MEMS). One of the basic steps in understanding physical aspects of many of these devices is scrutiny of the physical aspects of fluid flow and heat transfer in microchannels. In this respect, the analysis of the slip flows of combined free and force convection through vertical parallel plate microchannels, which have applications to many engineering fields, such as microelectrochemical cell transport, micro heat exchanging and microchip cooling, is of prime importance.

In contrast to the forced convection that has received proper attention in the literature [1–4], very limited information is available with regard to mixed convection in micro-systems. One of the early studies on the mixed convection in microchannels is carried out by Avci and Aydin [5] in which they analytically investigated the fully developed mixed convection in a vertical parallel-plate microchannel with constant wall temperatures. The same authors further extended their study [6] to microchannel with walls at uniform heat fluxes. Recently, Avci and Aydin [7] studied analytically the fully developed mixed convective heat transfer in a vertical microannulus between two concentric microtubes.

On the topic of the rarefaction effects on the natural convection, there are a few studies available in the literature. Chen and Weng [8] studied the fully developed natural convection in a vertical parallel-plate microchannel analytically. Biswal et al [9] numerically investigated the flow and heat transfer characteristics in the developing region of an isothermal microchannel. Recently, Buonomo and Manca [10] numerically investigated the steady-state developing natural convection in a vertical parallel-plate channel for asymmetric uniform heat fluxes at reduced pressure environment. To the best of our knowledge, no investigation has been made yet to analyze the developing mixed convective gas flows in microchannels. As a first study on this topic, the aim of the present study is to carry out a comprehensive computational study of mixed convective slip flow in the entrance and fully developed regions of a vertical open-ended parallel plate microchannel with symmetric and asymmetric uniform wall heat fluxes.

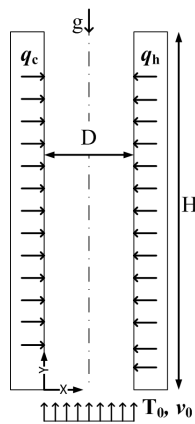


Fig. 1. Flow geometry and the coordinates system.

2. PROBLEM FORMULATIONS

Consider a vertical parallel plate channel and Cartesian coordinates x and y , as shown in Fig. 1. The channel height, H , is chosen fifty times larger than its width, D , to ensure the fully developed flow conditions at the channel exit. The ambient air at temperature T_0 with uniform velocity v_0 enters the channel. The microchannel walls are subjected to symmetrical or asymmetrical uniform and constant heat fluxes, which is more consistent with the heat generation process in chipsets as compared to constant surface temperature. Considering the common Boussinesq approximation, which is applicable to the present problem due to the relatively low temperature variations along the channel, the governing equations described by continuity, momentum and energy equations for a two dimensional, steady, laminar and incompressible flow are as follows:

$$\frac{\partial u}{\partial x} + \frac{\partial v}{\partial y} = 0, \quad (1)$$

$$\rho \left(u \frac{\partial u}{\partial x} + v \frac{\partial u}{\partial y} \right) = -\frac{\partial p}{\partial x} + \frac{\partial}{\partial x} \left(\mu \frac{\partial u}{\partial x} \right) + \frac{\partial}{\partial y} \left(\mu \frac{\partial u}{\partial y} \right), \quad (2)$$

$$\rho \left(u \frac{\partial v}{\partial x} + v \frac{\partial v}{\partial y} \right) = -\frac{\partial p}{\partial y} + \frac{\partial}{\partial x} \left(\mu \frac{\partial v}{\partial x} \right) + \frac{\partial}{\partial y} \left(\mu \frac{\partial v}{\partial y} \right) + \rho g \beta (T - T_0), \quad (3)$$

$$\rho \left(u \frac{\partial c_p T}{\partial x} + v \frac{\partial c_p T}{\partial y} \right) = \frac{\partial}{\partial x} \left(k \frac{\partial T}{\partial x} \right) + \frac{\partial}{\partial y} \left(k \frac{\partial T}{\partial y} \right) + \mu \left[2 \left\langle \left(\frac{\partial u}{\partial x} \right)^2 + \left(\frac{\partial v}{\partial y} \right)^2 \right\rangle + \left(\frac{\partial u}{\partial y} + \frac{\partial v}{\partial x} \right)^2 \right], \quad (4)$$

where β is volumetric thermal expansion coefficient, μ is dynamic viscosity, ρ is the density, c_p is specific heat at constant pressure and k is thermal conductivity. Consistent with the Boussinesq approximation the density is assumed to be constant and equal to 1.3 kg/m^3 . The viscous dissipation term is also included in the energy equation to examine its effect on the considered problem.

Based on gas kinetic theory, there is a non-zero velocity associated with the flow near channel walls in slip region, and the Maxwell slip model relates the velocity slip to the local velocity gradient at the wall according to [11]:

$$v_s = \frac{2 - \sigma_v}{\sigma_v} Kn D_h \left(\frac{\partial v}{\partial x} \right)_g. \quad (5)$$

For molecules that are not thermally accommodated with the wall, there is a temperature discontinuity known as temperature jump, which can be expressed according to gas kinetic theory as [12]:

$$T_s - T_w = \frac{2 - \sigma_t}{\sigma_t} \frac{2\gamma}{\gamma + 1} Kn D_h \left(\frac{1}{Pr} \frac{\partial T}{\partial x} \right)_g, \quad (6)$$

where T_s is the temperature of the gas layer adjacent to the wall, T_w is the wall temperature, γ is the specific heat ratio and $D_h = 2D$ is hydraulic diameter. Also, σ_v and σ_t are the tangential momentum and energy accommodation coefficients, which are determined experimentally. However, their values for most engineering applications are approximately around one [9], which is also adopted in the present study. For inlet boundary conditions, $u = 0$, $v = v_0$ and $T = T_0$ are assumed. For all flow variables at the outlet, zero gradients in the flow direction are applied except for the temperature gradient which is constant, consistent with the fixed applied heat fluxes. At walls, slip velocity and temperature jump conditions according to Eqs. (5) and (6) are employed. Corresponding to the constant wall heat flux condition, the normal temperature gradient is given and equal to:

$$\left(\frac{\partial T}{\partial x} \right)_g = \frac{q}{k}, \quad (7)$$

where q is the imposed heat flux. The local Nusselt number is evaluated according to:

$$Nu = \frac{q D_h}{(T_w - T_m) k}, \quad (8)$$

where the mean temperature is defined as:

$$T_m = \frac{\int_0^D v T dx}{\int_0^D v dx}. \quad (9)$$

The local friction coefficient at walls of the channel are defined as:

$$\Gamma = \frac{D_h}{\nu_0} \left(\frac{\partial v}{\partial x} \Big|_g \right). \quad (10)$$

3. NUMERICAL MODELING AND VALIDATIONS

The governing equations are solved using a finite volume approach. The convective terms are discretized using the power-law scheme, while for diffusive terms the central differencing is employed. Coupling between the velocity and pressure is made with SIMPLE algorithm [13]. The resulting system of the discretized linear algebraic equations is solved with an ADI scheme. The aforementioned solution scheme along with the SIMPLE algorithm have proved ability to model flows under the influence of the buoyancy effects with reasonable accuracy [9].

Extensive computations have been performed to identify the number of grid points that produces reasonably grid independent results. The quantity examined for this purpose is the average Nusselt number. Table 1 presents the grid resolution studies for the Nusselt number at $Kn = 0.05$ and $Gr/Re = 50$. Consequently, a system of 70×800 grid points with the expansion ratios of 1.022 and 1.006 is adopted for the cross sectional and axial directions, respectively. As for convergence of the iteration procedure, both of the following criteria must be met:

1. $[\Psi - \Psi_{old}] / \Psi_{max} \leq 10^{-5}$, where Ψ represents the variable for which the problem is solved at the current iteration, *old* represents the corresponding value at the previous iteration and Ψ_{max} is the maximum value of the variable in the entire domain.
2. The residual of the overall energy balance along all boundaries of the solution domain must be less than 1%.

Grid	Nu
35×800	5.42451
70×400	5.39284
70×800	5.33758
140×800	5.35261
70×1600	5.34241

Table 1. Grid resolution effects on the Nusselt number.

The numerical scheme has been validated by comparing the fully developed velocity and temperature profiles with the analytical solution of Avci and Aydin [6] as shown in Fig. 2(a,b), respectively. In the following, the non-dimensional temperature profiles of $\theta - \theta_w = \frac{T - T_{s,c}}{q_h D_h / k} - \frac{T_w - T_{s,c}}{q_h D_h / k}$ are plotted, which become invariant in the fully developed region. The flow parameters are the heat flux ratio, $r_q = q_c / q_h$, the modified mixed convection parameter, $Gr/Re = 50$, and Knudsen numbers of 0, 0.05 and 0.1. The axial velocity and length are nondimensionalized by the inlet velocity, ν_0 , and the hydraulic diameter, D_h , respectively. Fully developed velocity and temperature profiles obtained numerically are in good agreement with the corresponding analytical results of Avci and Aydin [6].

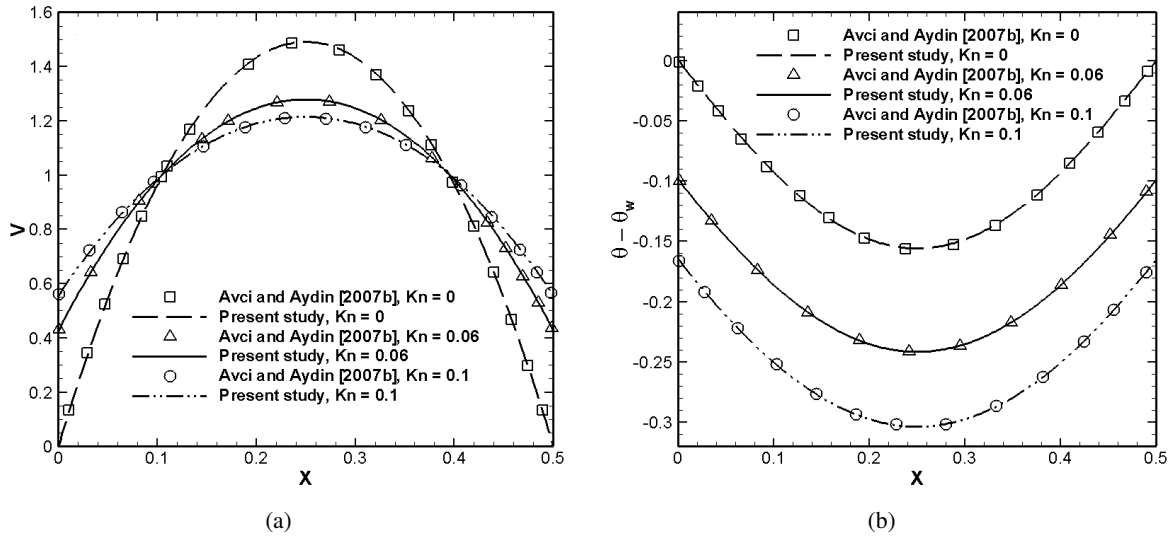


Fig. 2. Comparison of the fully developed (a) velocity and (b) temperature profiles with those of Avci and Aydin [6] at $r_q = 1$; $Gr/Re = 50$; $Kn = 0, 0.06$ and 0.1 .

4. RESULTS AND DISCUSSION

The mixed convection parameter, $\frac{Gr}{Re} = \left(\frac{\rho^2 \beta g q_h D_h^4}{k \mu^2} \right) / \left(\frac{\rho v_0 D_h}{\mu} \right)$, is a nondimensional parameter, which indicates the relative importance of natural convection over forced convection and governs the mixed convection flow [6], and will be used in presenting the results. All thermo-physical properties are evaluated at the inlet air temperature of $T_0 = 273.15$ K. The volumetric thermal expansion coefficient, β , is obtained according to the ideal gas approximation. The slip flow regime, $0.001 \leq Kn \leq 0.1$, is considered, which is typical in microdevices, since their length scales are in the range of 1–100 μm and the mean free path of air molecules at atmospheric condition is in the order of 0.1 μm [14]. The applied hot wall heat fluxes are ranging from 30 to 60 W/m^2 , corresponding to a range of the Gr/Re from 10 to 100, which models the physical and meaningful range of fluid temperatures along the channel. The cold wall heat flux, q_c , is determined based on the hot wall heat flux, q_h , and the specified heat flux ratio, r_q . The effects of Knudsen number, heat flux ratio, $0 \leq r_q \leq 1$, and mixed convection parameter on the fluid flow and heat transfer through a vertical parallel plate channel with symmetric and asymmetric wall heat fluxes are examined.

The developments of velocity profiles in axial and cross sectional directions are presented in Figs. 3 and 4, respectively. Both the axial and cross sectional coordinates and axial velocity are normalized with respect to the hydraulic diameter and the inlet velocity, respectively. Velocity profiles are plotted for $Kn = 0.05$, $Gr/Re = 100$, and $r_q = 0.2$. It is observed from Fig. 3 that as the fluid in the channel heats up, the point of maximum velocity shifts toward the hot wall, due to the buoyancy effects, which impose an upward flow in the close vicinity of the hot wall. It is important to note here that the buoyancy force is almost negligible close to the channel inlet, and gains weight along the channel as the fluid temperature increases and reduces the fluid density. A cross flow field, $U = \frac{uRe}{v_0}$, is formed close to the entrance region because of the uniform inlet velocity profile and the dragging effects of the walls as shown in Fig. 4. The positive cross-flow field is stronger than the negative field, which is a direct consequence of the mass conservation and the higher axial velocities near the hot wall.

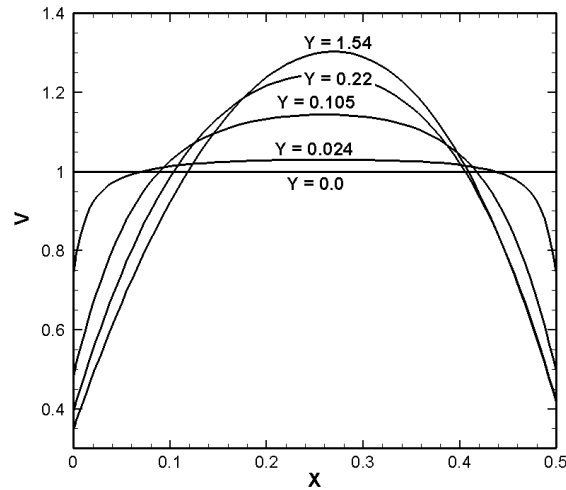


Fig. 3. Streamwise velocity profiles at different axial locations for $Gr/Re = 100$, $Kn = 0.05$ and 1.

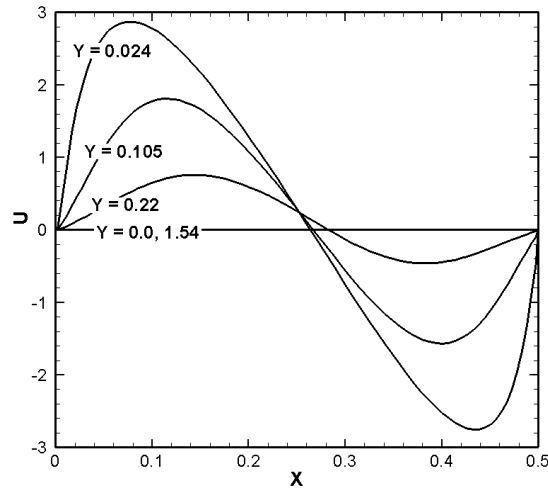


Fig. 4. Cross-flow velocity profiles at different axial locations for $Gr/Re = 100$, $Kn = 0.05$ and 1.

The effects of Knudsen number and mixed convection parameter on the axial variations of slip velocities are presented in Fig. 5. As indicated by Eq. (5), the velocity slip is directly related to the Kn , and therefore, increases at higher Knudsen numbers. For a constant temperature ratio of $r_q = 1$, increasing Gr/Re at a given Kn results in stronger buoyancy effects and increases velocity gradients near the walls, which in turn leads to an increase in slip velocities.

The effects of heat flux ratio, r_q , on the axial variations of slip velocities at hot and cold walls are illustrated in Fig. 6(a,b) for $Gr/Re = 100$. Decreasing r_q shifts the maximum axial velocity toward the hot wall, leading to higher and lower slip velocities on the hot and cold walls, respectively. The slight increase in the slip velocities after their initial drops in Fig. 6(b) can be explained as follows. In the entry region of the channel due to asymmetrical temperature distributions in cases with $r_q \neq 1$, the buoyancy force increases the velocity gradients near the hot wall. This effect, which is stronger at lower r_q and higher values of Knudsen number, results in the slight slip velocity increase near the hot wall.

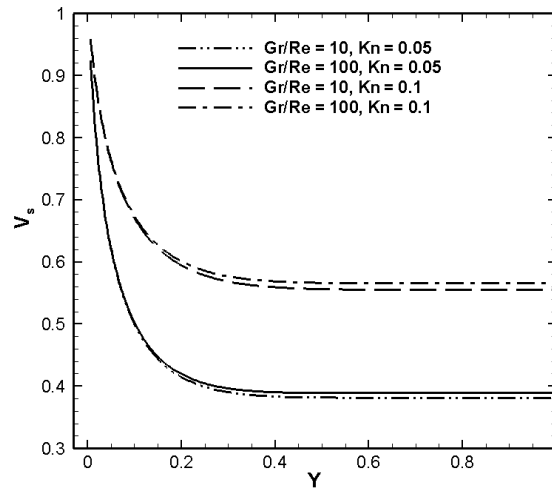


Fig. 5. Axial variations of slip velocities for $r_q = 1$ and different values of Gr/Re and Kn .

Figure 7 exhibits the developments of the non-dimensional temperature field, $\theta - \theta_{cw} = \frac{T - T_{s,c}}{q_h D_h / k} - \frac{T_{cw} - T_{s,c}}{q_h D_h / k}$, along the channel for flow conditions the same as those in Figs. 3 and 4. Clearly, the temperature of the hot wall continuously increases along the channel, as the minimum temperature moves toward the cold wall.

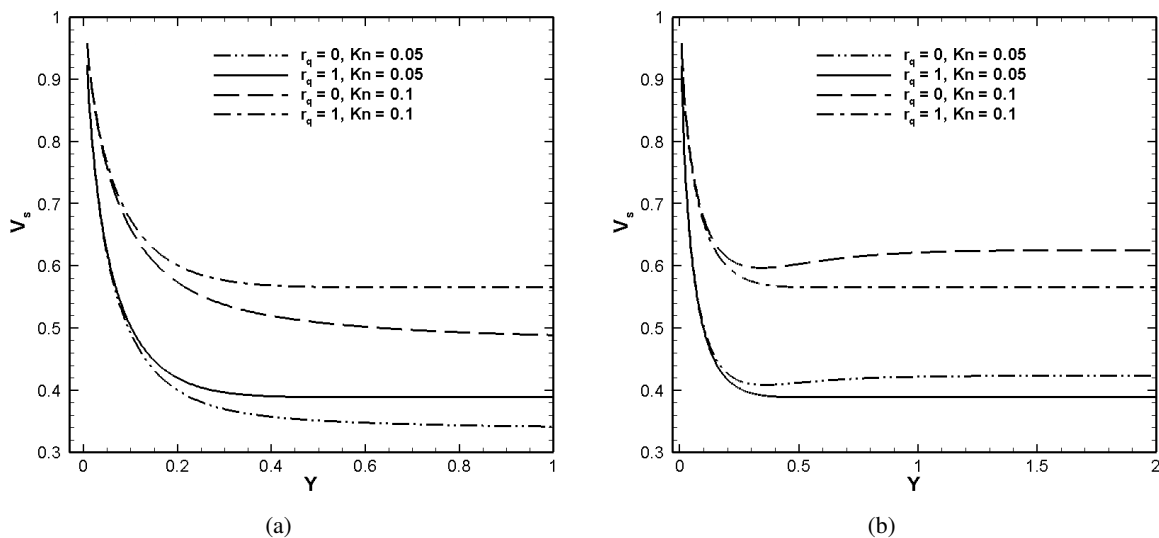


Fig. 6. Axial variations of slip velocities along (a) the cold wall; and (b) the hot wall for $Gr/Re = 100$ and different values of r_q and Kn .

Figures 8(a,b,c) illustrate, respectively, the effects of the mixed convection parameter on the axial and cross sectional velocity, and temperature profiles. As for the axial velocity profiles, buoyancy effects increase the velocities near the hot wall. In the early sections of the channel the velocity profiles are slightly influenced by the buoyancy force. However, as the fluid heats up and the buoyancy force gains weight along the channel, the velocity profiles move toward the hot wall. This motion is more prominent at higher mixed convection parameter. Figure 8(a) also shows that the velocity slip intensely increases near the hot wall at higher mixed convection parameter. Figure 8(b) indicates that the cross flow velocities strongly influ-

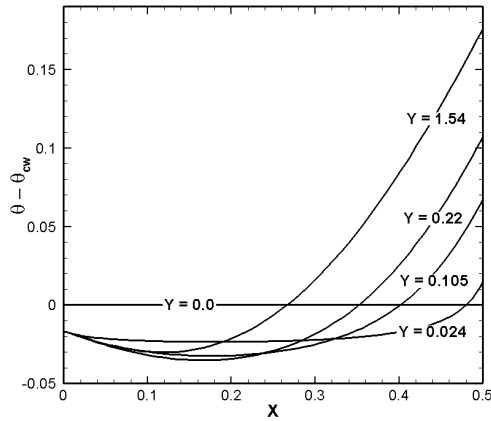


Fig. 7. Cross sectional temperature profiles at different axial locations for $Gr/Re = 100$, $Kn = 0.05$ and $r_q = 0.2$.

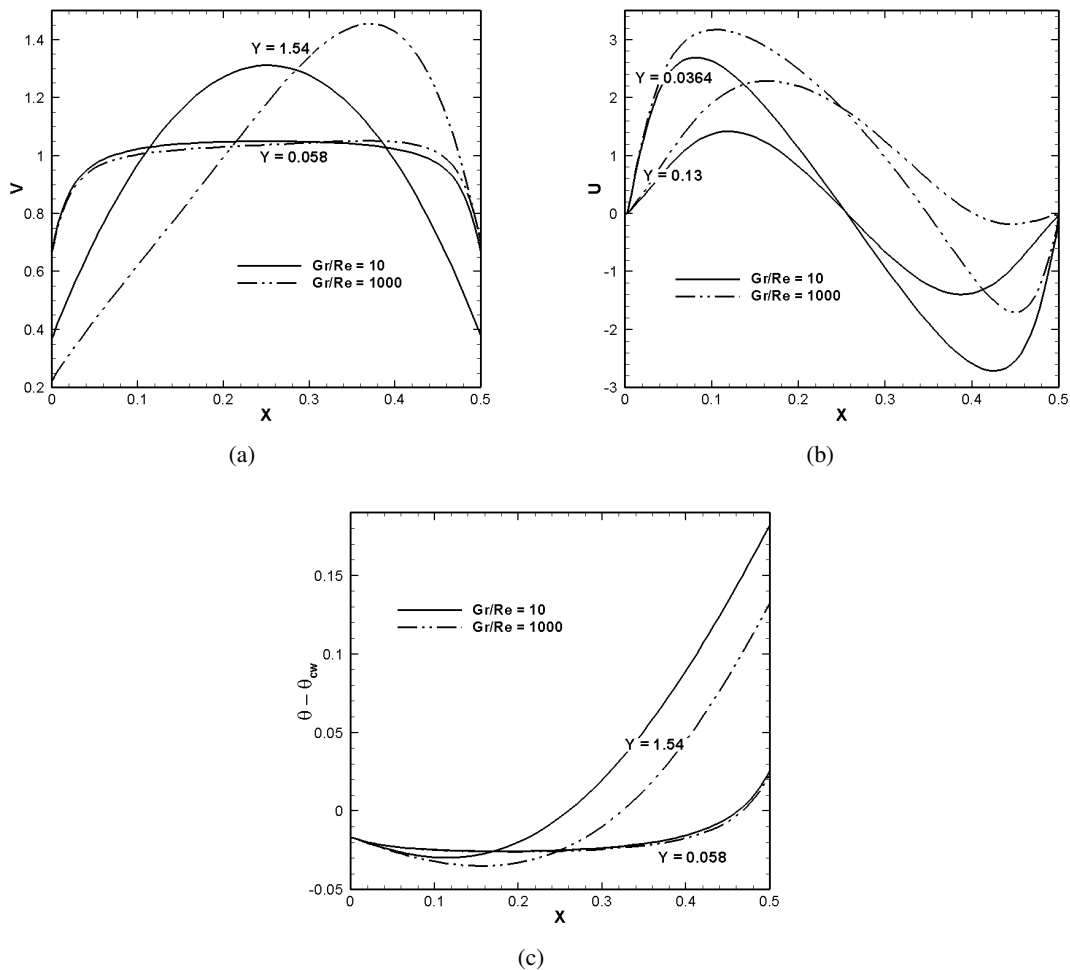


Fig. 8. Effects of mixed convection parameter on the (a) axial velocity; (b) cross flow velocity; and (c) temperature profiles for $Kn = 0.05$ and $r_q = 0.2$.

enced by the buoyancy force. Their values dramatically increase, and the profiles mostly become positive for higher mixed convection parameter. Consistent with the axial velocity profiles in Fig. 8(a), the temperature profiles are not influenced by mixed convection parameter at the early section of the channel, where the buoyancy effects are negligible as shown in Fig. 8(c). However, as the axial velocity near the hot wall increases at higher mixed convection parameter (see Fig. 8a), the fluid temperature decreases there.

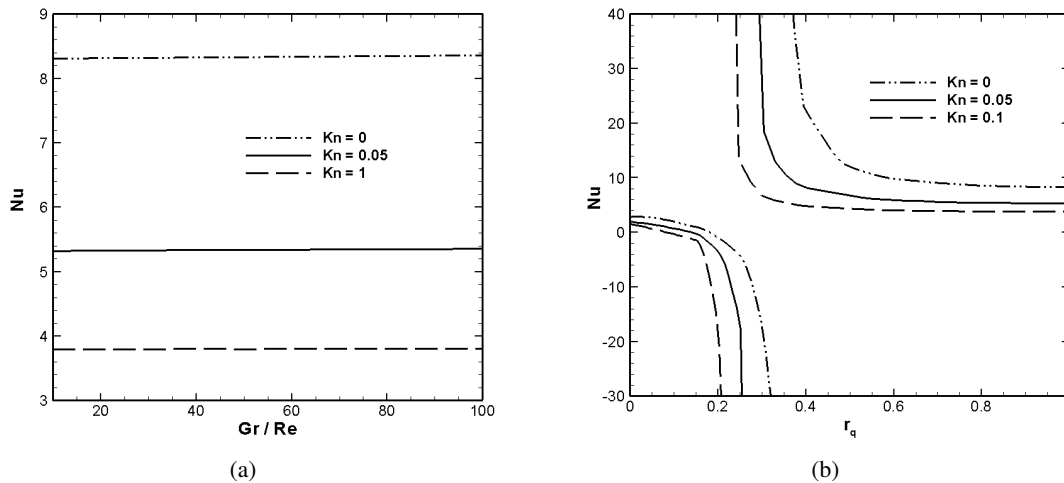


Fig. 9. The variations of the average Nusselt number with (a) Gr/Re for $r_q = 1$; and (b) r_q for $Gr/Re = 100$, and different values of Kn .

The effects of buoyancy force and heat flux ratio on the average Nusselt number at different values of Kn are shown in Fig. 9(a,b). The heat transfer rate decreases with an increase in Kn number, as evident from Fig. 9(a). Also, increasing mixed convection parameter slightly increases the heat transfer rate. It is observed from Fig. 9(b) that Nu displays a discontinuity with a vertical asymptote. Left to this point, Nu is first positive, becoming zero, and finally obtains a negative value, whereas on the right, Nu is always positive. It is observed that this discontinuity occurs when the mean temperature reaches the temperature of the cold wall and the denominator in the definition of Nu_c becomes zero. Therefore, there is an undefined point in the heat transfer rate. The values of the heat flux ratio for occurring these undefined points decreases with increasing Kn number.

For more clarification, the axial variations of heat transfer rate, Nu , along the hot and cold walls for $Gr/Re = 100$, $r_q = 0.3$ and several values of the Kn numbers are plotted in Fig. 10(a,b), respectively. It can be seen that the Nusselt number decreases with an increase in Knudsen number. Despite the fact that the Nusselt number of the hot wall is always positive and continuously decreasing along the channel, the Nusselt number of the cold wall exhibits totally different behavior. It is observed that the Nu_c has a discontinuity point at $Kn = 0$. However, heat transfer rate is positive and continuously increasing along the channel at the $Kn = 0.05$ and 1.

Figure 11(a,b) depicts the effects of buoyancy force and heat flux ratio on the average friction coefficient at different values of Kn . As expected at higher Knudsen numbers the friction coefficient reduces dramatically due to the slip effects. However, increasing in mixed convection parameter and heat flux ratio slightly increase the friction coefficient, which is more noticeable at lower Kn numbers.

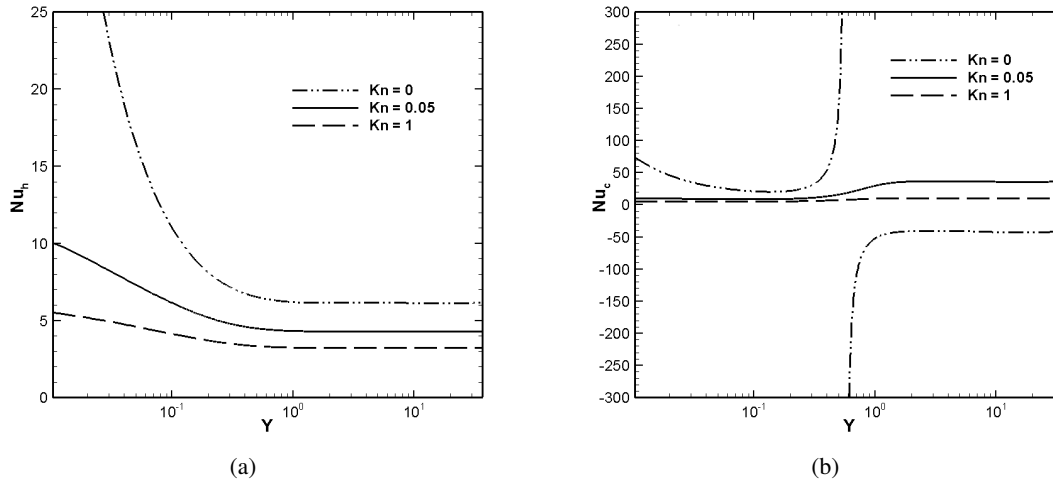


Fig. 10. Variations of local Nusselt number along (a) the hot wall; and (b) the cold wall for $r_q = 0.3$, $Gr/Re = 100$ and different values of Kn .

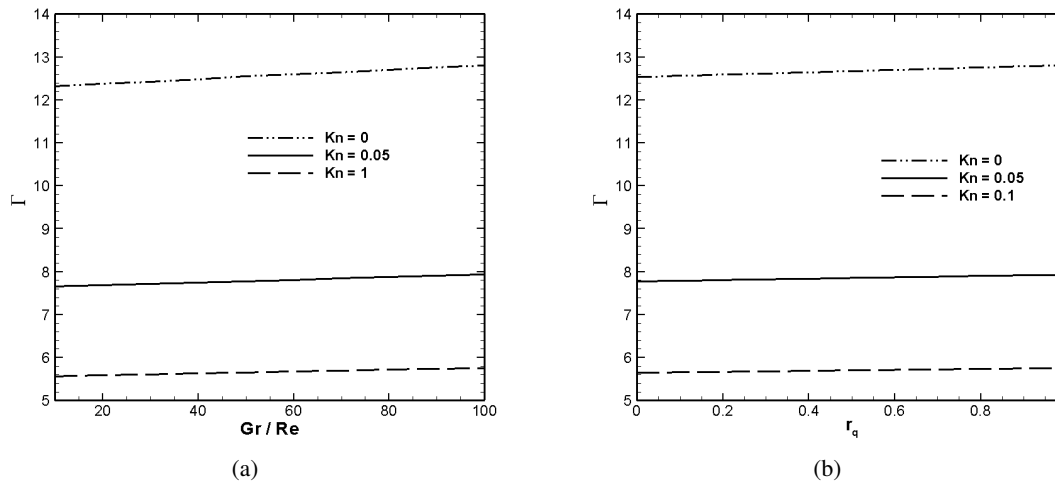


Fig. 11. The variations of the average friction coefficient with (a) Gr/Re for $r_q = 1$; and (b) r_q for $Gr/Re = 100$, and different values of Kn .

5. CONCLUSIONS

A numerical analysis on the developing and developed mixed convective slip flows through a symmetric and asymmetric heated vertical channel has been performed. The governing equations subject to the slip/jump boundary conditions are solved using a control volume technique. The numerical scheme validation was established through comparison of the numerical velocity and temperature profiles with their analytical counterparts. The effects of rarefaction, buoyancy and temperature ratio on both developing and fully developed velocity and temperature profiles are examined in details. The major findings of the present study can be summarized as follows:

1. Slip velocity on the hot wall increases with increasing Gr/Re and decreasing r_q , while the opposite effects are observed on the cold wall.

2. The cross flow velocities strongly influenced by the buoyancy force. Their values dramatically increase for higher mixed convection parameter.
3. Increasing Gr/Re leads to an increase in the heat transfer rate. In addition, rarefaction effects decrease the heat transfer rate.
4. The friction coefficient decreases with an increase in Kn and heat flux ratio and a decrease in mixed convection parameter.
5. There are undefined points in the heat transfer rate at some heat flux ratios. The heat flux ratio for occurring these undefined points decreases with increasing Kn number.

ACKNOWLEDGEMENTS

The authors gratefully acknowledged the financial support of Ferdowsi University of Mashhad under research Grant No. 2/16829.

REFERENCES

1. Morini, G.L. and Spiga M., "The role of the viscous dissipation in heated micro-channels", *Journal of Heat Transfer*, Vol. 129, No. 3, pp. 308–318, 2007.
2. Dongari, N. and Agrawal, A., "Analytical solution of gaseous slip flow in long microchannels", *International Journal of Heat and Mass Transfer*, Vol. 50, Nos. 17–18, pp. 3411–3421, 2007.
3. Qazi Zade, A., Ahmadzadegan, A. and Renksizbulut, M., "A detailed comparison between Navier-Stokes and DSMC simulations of multicomponent gaseous flow in microchannels", *International Journal of Heat and Mass Transfer*, Vol. 55, Nos. 17–18, pp. 4673–4681, 2012.
4. Bahrami, H., Bergman, T.L. and Faghri, A., "Forced convective heat transfer in a microtube including rarefaction, viscous dissipation and axial conduction effects", *International Journal of Heat and Mass Transfer*, Vol. 55, Nos. 23–24, pp. 6665–6675, 2012.
5. Avci, M. and Aydin, O., "Mixed convection in a vertical parallel plate microchannel", *Journal of Heat Transfer*, Vol. 129, No. 2, pp. 162–166, 2007.
6. Avci, M. and Aydin, O., "Mixed convection in a vertical parallel plate microchannel with asymmetric wall heat fluxes", *Journal of Heat Transfer*, Vol. 129, No. 8, pp. 1091–1095, 2007.
7. Avci, M. and Aydin, O., "Mixed convection in a vertical microannulus between two concentric microtubes", *Journal of Heat Transfer*, Vol. 131, No. 1, pp. 014502–4, 2009.
8. Chen, C. K. and Weng, H. C., "Natural convection in a vertical microchannel", *Journal of Heat Transfer*, Vol. 127, No. 9, pp. 1053–1056, 2005.
9. Biswal, L., Som, S. K. and Chakraborty, S., "Effects of entrance region transport processes on free convection slip flow in vertical microchannels with isothermally heated walls", *International Journal of Heat and Mass Transfer*, Vol. 50, Nos. 7–8, pp. 1248–1254, 2007.
10. Buonomo, B. and Manca, O., "Natural convection slip flow in a vertical microchannel heated at uniform heat flux", *International Journal of Thermal Sciences*, Vol. 49, No. 8, pp. 1333–1344, 2010.
11. Maxwell, J. C., "On stress in rarefied gases from inequalities of temperature", *Philosophical Transactions of the Royal Society of London*, Vol. 170, pp. 231–256, 1879.
12. Kennard, E., *Kinetic Theory of Gases*, McGraw-Hill Book Co., New York, 1938.
13. Patankar, S. V., *Numerical Heat Transfer and Fluid Flow*, McGraw-Hill, New York, 1980.
14. Karniadakis, G. and Beskok, A., *Micro Flows*, Springer-Verlag, Berlin, 2002.